

# Dynamic Blood–Brain Barrier Regulation in Mild Traumatic Brain Injury

Eoin O’Keeffe,<sup>1,\*</sup> Eoin Kelly,<sup>2,\*</sup> Yuzhe Liu,<sup>3</sup> Chiara Giordano,<sup>3</sup> Eugene Wallace,<sup>2</sup> Mark Hynes,<sup>4</sup> Stephen Tiernan,<sup>5</sup> Aidan Meagher,<sup>5</sup> Chris Greene,<sup>1</sup> Stephanie Hughes,<sup>6</sup> Tom Burke,<sup>7</sup> John Kealy,<sup>1</sup> Niamh Doyle,<sup>6</sup> Alison Hay,<sup>2</sup> Michael Farrell,<sup>8</sup> Gerald A. Grant,<sup>9</sup> Alon Friedman,<sup>10,11</sup> Ronel Veksler,<sup>10</sup> Michael G. Molloy,<sup>12</sup> James F. Meaney,<sup>13,14</sup> Niall Pender,<sup>6</sup> David Camarillo,<sup>3,\*</sup> Colin P. Doherty,<sup>2,7,\*</sup> and Matthew Campbell<sup>1,\*</sup>

## Abstract

Whereas the diagnosis of moderate and severe traumatic brain injury (TBI) is readily visible on current medical imaging paradigms (magnetic resonance imaging [MRI] and computed tomography [CT] scanning), a far greater challenge is associated with the diagnosis and subsequent management of mild TBI (mTBI), especially concussion which, by definition, is characterized by a normal CT. To investigate whether the integrity of the blood–brain barrier (BBB) is altered in a high-risk population for concussions, we studied professional mixed martial arts (MMA) fighters and adolescent rugby players. Additionally, we performed the linear regression between the BBB disruption defined by increased gadolinium contrast extravasation on dynamic contrast-enhanced magnetic resonance imaging (DCE-MRI) on MRI and multiple biomechanical parameters indicating the severity of impacts recorded using instrumented mouthguards in professional MMA fighters. MMA fighters were examined pre-fight for a baseline and again within 120 h post-competitive fight, whereas rugby players were examined pre-season and again post-season or post-match in a subset of cases. DCE-MRI, serological analysis of BBB biomarkers, and an analysis of instrumented mouthguard data, was performed. Here, we provide pilot data that demonstrate disruption of the BBB in both professional MMA fighters and rugby players, dependent on the level of exposure. Our data suggest that biomechanical forces in professional MMA and adolescent rugby can lead to BBB disruption. These changes on imaging may serve as a biomarker of exposure of the brain to repetitive subconcussive forces and mTBI.

**Keywords:** blood–brain barrier; blood–brain barrier dysfunction; MRI

## Introduction

**T**RAUMATIC BRAIN INJURY (TBI) is the leading cause of death in children and young adults globally. Indeed, the incidence of TBI can be considered to have reached epidemic proportions, and there have been few recent advances for the treatment of malignant brain swelling that may evolve after severe TBI.<sup>1,2</sup> If brain swelling persists, the risks of permanent brain damage or mortality are

greatly increased.<sup>3</sup> Whereas TBI is a relative risk in modern contact sports, the number of deaths and major disabilities originating from sports-related severe TBI are small. A far greater challenge is the occurrence of repetitive mild TBI (mTBI), commonly referred to as concussive or sometimes subconcussive injuries.<sup>4</sup>

Generally, mTBI can be classified as injury to the brain resulting from blunt trauma or acceleration/deceleration of the head and neck with one or more of the following conditions attributable

<sup>1</sup>Smurfit Institute of Genetics, Trinity College Dublin, Dublin, Ireland.

<sup>2</sup>Department of Neurology, Health Care Centre, Hospital 5, St. James’s Hospital, Dublin, Ireland.

<sup>3</sup>Department of Mechanical Engineering, Stanford University, Stanford, California.

<sup>4</sup>Personal Health, Dublin, Dublin, Ireland.

<sup>5</sup>Department of Mechanical Engineering, Technological University Dublin, Dublin, Ireland.

<sup>6</sup>Department of Psychology, Beaumont Hospital, Dublin, Ireland.

<sup>7</sup>Academic Unit of Neurology, Biomedical Sciences Institute, Trinity College Dublin, Dublin, Ireland.

<sup>8</sup>Department of Neuropathology, Beaumont Hospital, Dublin, Ireland.

<sup>9</sup>Department of Neurosurgery, Stanford University School of Medicine, Stanford, California.

<sup>10</sup>Department of Cognitive and Brain Sciences, Zlotowski Center for Neuroscience, Ben-Gurion University of the Negev, Beer-Sheva, Israel.

<sup>11</sup>Department of Medical Neuroscience, Dalhousie University, Halifax, Nova Scotia, Canada.

<sup>12</sup>Department of Medicine, University College Cork, Cork, Ireland.

<sup>13</sup>Department of Radiology, St. James’s Hospital, Dublin, Ireland.

<sup>14</sup>Centre for Advanced Medical Imaging (CAMI), St. James’ Hospital, Dublin, Ireland.

\*These authors contributed equally.

to the TBI during the post-traumatic surveillance period: 1) any period of observed or self-reported transient confusion, disorientation, or impaired consciousness; 2) any period of observed or self-reported dysfunction of memory (amnesia) around the time of injury; and 3) observed signs of other neurological or neuropsychological dysfunction, such as seizures in the immediate aftermath of TBI, headache, dizziness, irritability, fatigue, or poor concentration.<sup>5</sup>

In the context of participation in contact sports, there are frequently challenges in getting an accurate diagnosis and appropriate treatment post-concussion, especially when there is no documented or observed loss of consciousness or symptom complex that is easily recognized. Additionally, it must be recognized that there does not need to be any subjective clinical signs or symptoms for a brain injury to have occurred. In that regard, the nature of certain sports such as American football, rugby, and boxing are such that repetitive exposure of the head to what is termed subconcussive forces may lead to an accumulation of silent damage to distinct brain regions.<sup>6–8</sup> However, current acute standard of care imaging with magnetic resonance imaging (MRI) is often not sensitive enough to pick up any damage, and the underlying pathophysiology of these subconcussive forces is far from established in human mTBI. Similarly, imaging paradigms after chronic exposure to mTBI is faced with similar challenges.

The exposure of children and young adults to sports that involve an increased risk of TBI is controversial. We do know that boxing fighters suffer repeated mTBI episodes and are at risk of permanent brain damage and chronic traumatic encephalopathy (CTE).<sup>9,10</sup> Although CTE is well known to be present in fighters and other professional contact athletes, there are far less data on the risks for children in contact sports.<sup>11</sup>

We and others recently reported, for the first time, that blood–brain barrier (BBB) dysfunction is associated with pathology of CTE.<sup>12,13</sup> The BBB plays a critical role in maintaining central nervous system (CNS) homeostasis.<sup>14</sup> Such is the impact of the BBB on neural integrity that it can be estimated that each neuron is perfused by its own capillary, with no neuron being further than  $\sim 25 \mu\text{m}$  from a capillary. Indeed, the combined surface area of cerebral microvessels is 150–200  $\text{cm}^2/\text{g}$  of brain tissue, which equates to approximately 15–20  $\text{m}^2$  per adult human brain.<sup>15–18</sup>

Given that BBB integrity is readily assessed in human subjects, we have sought to understand the character, mechanism, and structural/functional consequences of exposure to TBIs in two age groups. We prospectively followed professional mixed martial arts (MMA) fighters and adolescent rugby union players.

Surprisingly, we found evidence of dynamic BBB disruption in a subset of adolescents exposed to a season (6 months) of rugby union in the absence of diagnosed concussion. This disruption was measured with enhanced gadolinium signal and occurred in tandem with a distinct set of serological readouts that may allow for an objective measure of neural damage to be assessed. In 5 professional MMA fighters who were all diagnosed with a concussion, we observed a wide spectrum of BBB integrity. Instrumented mouthguards were used to measure fighters' head kinematics. The mouthguards were previously developed and extensively validated for measuring head kinematics in American football games.<sup>19,20</sup> The linear regressions between parameters representing the impact exposures and the resulting BBB disruption were performed. Some of the parameters show good correlations, which suggested a potential means of assessing damage to the concussed brain. Specifically, we found that, within a given match, the maximum deformation (strain and strain rate) that the brain experienced over all impacts correlated well with BBB disruption.

## Methods

### *Traumatic brain injury measurements and brain tissue deformation estimations*

We deployed the Stanford Instrumented Mouthguard (MiG2.0) to 5 professional MMA fighters during regular matches ( $n=5$  subjects, six fights). The human subject protocol was approved by the Stanford, Trinity College and Institute of Technology Tallaght Panel for the Protection of Human Subjects. We conducted data collection in accord with the institutional review boards' guidelines and regulations. Both video analysis and instrumented mouthguard data were used to validate each impact.

The MiG2.0 senses 6 degrees of freedom (6DOF) kinematics by a triaxial accelerometer and a triaxial gyroscope. The sensory board is completely sealed between three layers of ethylene vinyl acetate (EVA) material, and communication occurs by blue-tooth. A tight fit to the dentition is achieved by forming the EVA material around a dental model.<sup>19</sup> In this study, we recorded events with linear acceleration exceeding 10 g in agreement with previously published systems.<sup>20</sup> The acquisition window was 50 ms pre-trigger and 150 ms post-trigger. Linear acceleration and angular velocity were filtered using a fourth-order Butterworth low-pass filter with cut-off frequency of 300 Hz. Angular acceleration was estimated using a 5-point stencil derivative of the measured angular velocity. The instrumented mouthguard is well validated in football applications.<sup>19,20</sup> To validate it in MMA applications, we reproduced a similar loading (peak of  $\sim 150$  g and duration of  $\sim 5$  ms) on a hybrid III dummy head in the lab, and the kinematics measured matched well with the sensors at center of gravity of the head. The mouthguard will give high linear and angular acceleration when the sensors are directly impacted or the mouthguard is not rigidly fit to the teeth.

Estimates of brain tissue deformation for all TBIs were obtained from simulations using the KTH finite element (FE) model (KTH Royal Institute of Technology, Stockholm, Sweden).<sup>21,22</sup> This model includes the brain, skull, scalp, meninges, cerebrospinal fluid (CSF), and 11 pairs of bridging veins. Skull acceleration measured from the MiG2.0 was prescribed to follow the measured 6DOF head accelerations, and ensuing brain deformation was observed. The brain was modeled as an Ogden hyperelastic constitutive material to account for large deformations of the tissue, with additional linear viscoelastic terms to account for the rate dependence of the tissue. The boundary condition between the dura and skull was tied. Between the brain and dura, a sliding interface was implemented that allowed tangential, and not radial, movement between the structures (given the incompressibility of the mostly water CSF). The determined brain geometry and material properties were validated against displacement data from cadaver TBI experiments where neutral density targets were inserted inside cadaver brains and tracked using high-speed biplane X-ray during impacts.<sup>23,24</sup>

To locally compare brain deformation to BBB disruption from dynamic contrast enhanced (DCE)-MRI images, we implemented a protocol involving FE mesh voxelization and an affine registration between the DCE brain mask and the voxelized FE brain mask. First, the FE brain mesh was voxelized to obtain a reference volume (MATLAB R2018a; The MathWorks, Inc., Natick, MA); subsequently, a spatial transformation was used to align the DCE-MRI brain to the model. The volume resampling was performed with the three-dimensional (3D) SLICER 4.10.0 BRAIN registration package. Based on spatial coordinates, the mechanical deformation was assigned to the DCE-MRI voxels belonging to the corresponding element, and the mask of BBB disruption was selected using the threshold of slope reported in previous study.<sup>37</sup> Only the voxels with BBB disruption were considered in the linear regression.

The mechanical fields of the 1st principal strain ( $\epsilon$ ), the 1st principal strain rate ( $\dot{\epsilon}$ ), the 1st principal stress ( $\sigma$ ) and the energy absorption ( $\omega$ ) are based on 5 variables (time, impact, 3-dimensional space in the brain). Different methods were used to calculate

parameters to represent the severity of brain deformation during the game. As examples of  $\epsilon$  shown in Eqs. 1–6, the peak (superscript P) and the integration (superscript I) over history ( $t$ ) of  $\epsilon(t, im, x, y, z)$  were calculated for every voxel in the brain for each impact. Then, to take into account the effect of the multiple impacts, the maximum values over all impacts ( $im$ ) were calculated by Eq. 7 for every voxel in the brain to plot the maps in Fig. 1e (only the mask of BBB disruption is plotted). For the linear regression, statistical parameters are calculated as Total (subscript  $\Sigma$ ), Average (subscript A) and 95% (subscript 95) over the voxels ( $x, y, z$ ) in the mask of BBB disruption in the brain (above the threshold). The following equations describe the calculation for the 1<sup>st</sup> principal strain scalar parameters; the strain rate, principal stress, and energy absorbed are calculated using the same methods.

$$\epsilon_{\Sigma}^I = \Sigma_{(x,y,z)} \left( \text{Max}_{im} \left( \int_t \epsilon(t, im, x, y, z) \cdot dt \right) \right) \quad \text{Eq.1}$$

$$\epsilon_{\Sigma}^P = \Sigma_{(x,y,z)} (\text{Max}_{im}(\text{Max}_t(\epsilon(t, im, x, y, z)))) \quad \text{Eq.2}$$

$$\epsilon_A^I = \Sigma_{(x,y,z)} \left( \text{Max}_{im} \left( \int_t \epsilon(t, im, x, y, z) \cdot dt \right) \right) / V_D \quad \text{Eq.3}$$

$$\epsilon_A^P = \Sigma_{(x,y,z)} (\text{Max}_{im}(\text{Max}_t(\epsilon(t, im, x, y, z)))) / V_D \quad \text{Eq.4}$$

$$\epsilon_{95}^I = \text{Max}_{95(x,y,z)} \left( \text{Max}_{im} \left( \int_t \epsilon(t, im, x, y, z) \cdot dt \right) \right) \quad \text{Eq.5}$$

$$\epsilon_{95}^P = \text{Max}_{95(x,y,z)} (\text{Max}_{im}(\text{Max}_t(\epsilon(t, im, x, y, z)))) \quad \text{Eq.6}$$

$$\epsilon^P = \text{Max}_{im} (\text{Max}_t(\epsilon(t, im, x, y, z))) \quad \text{Eq.7}$$

Where  $\epsilon(t, im, x, y, z)$  is the strain at voxel ( $x, y, z$ ), at time point  $t$ , in the impact  $im$ .  $\text{Max}_i()$  is to calculate the maximum value over parameter  $i$ .  $\Sigma_i()$  is to calculate the total value over parameter  $i$ .  $\text{Max}_{95}()$  is to calculate the 95% value over parameter  $i$ .  $V_D$  is the volume of BBB disruption in the brain.  $\epsilon$  can be also replaced by  $\dot{\epsilon}$ ,  $\sigma$ ,  $\omega$  to calculate the parameters in Table 1 and Figure 1. The maximum peak values of the magnitude of linear (a) and angular ( $\alpha$ ) acceleration were calculated as an example shown in Eq. 8.

$$a^P = \text{Max}_{im}(\text{Max}_t(a)) \quad \text{Eq.8}$$

### Magnetic resonance imaging

All ethical approvals were in place before initiation of studies on human subjects. Initially, 22 participants were recruited pre-season for the schoolboy study; however, only 11 returned for post-season evaluation. All participants underwent a pre-season scan before the start of the competitive rugby season and underwent a post-season scan within 2 months of the end of the season in the case of the schoolboy team ( $n=11$ ). In addition, the university-based team participants (initially  $n=10$  recruited, but only  $n=8$  were scanned post-match) underwent a scan within 2 h of playing a full contact competitive rugby match. BBB permeability maps were created using the slope of contrast agent concentration in each voxel over time, calculated by a linear fit model as previously described. Thresholds of high permeability was defined by the 95th percentile

of all slopes in a previously examined control group.<sup>25</sup> Supra-threshold values of individuals were then normalized to pre-season values to determine relative change over the course of play. MMA fighters were scanned pre-fight and again within 120 h post-competitive fight using identical parameters as that used in the university-based rugby players.

All imaging was performed using a 3T Philips Achieva scanner (Philips, Best, The Netherlands) and included a T1-weighted (T1w) anatomical scan (3D gradient echo, echo time [TE]/repetition time [TR]=3/6.7 ms, acquisition matrix  $268 \times 244$ , voxel size:  $0.9 \times 0.9 \times 0.9$  mm), T2-weighted (T2w) imaging (TE/TR=80/3000 ms, voxel size:  $0.45 \times 0.45 \times 0.4$  mm), fluid-attenuated inversion recovery (FLAIR; TE/TR=125/11000 ms, voxel size:  $0.45 \times 0.45 \times 4$  mm).

In the first cohort, the calculation of pre-contrast longitudinal relaxation time ( $T_{10}$ ), the variable flip angle (VFA) method was used (3D T1w-FFE [fast field echo], TE/TR=2.78/5.67 ms, acquisition matrix:  $240 \times 184$ , voxel size:  $0.68 \times 0.68 \times 5$  mm, flip angles: 2, 10, 16, and 24 degrees). DCE sequence was then acquired (axial, 3D T1w-FFE, TE/TR=2.8/5.7 ms, acquisition matrix:  $240 \times 123$ , voxel size:  $1 \times 1.3 \times 5.0$  mm, flip angle: 6 degrees,  $\Delta t = 6.4$  sec, temporal repetitions: 70, total scan length: 7.43 min). An intravenous bolus injection of the contrast agent, gadobentate dimeglumine (Gd-BOPTA; Bracco Diagnostics Inc., Milan, Italy), was administered using an automatic injector after the first three DCE repetitions.

For the second, older cohort, T1w, T2w, and FLAIR imaging parameters were kept the same. For the calculation of pre-contrast longitudinal relaxation time ( $T_{10}$ ), the VFA method was used (3D T1w-FFE, TE/TR=3.1/6.5 ms, acquisition matrix:  $268 \times 244$ , voxel size:  $0.896 \times 0.896 \times 0.96$  mm, flip angles: 10, 15, 20, 25, and 30 degrees). DCE sequence was then acquired (axial, 3D T1w-FFE, TE/TR=1.8/5.0 ms, acquisition matrix:  $208 \times 144$ , voxel size:  $1.06 \times 1.17 \times 6.0$  mm, flip angle: 20 degrees,  $\Delta t = 20.2$  sec, temporal repetitions: 61, total scan length: 20.30 min). Intravenous bolus injection of the contrast agent, Gd-BOPTA, was administered using an automatic injector after the first five DCE repetitions.

To obtain permeability values in healthy individuals, we (co-author, Prof. Alon Friedman's group) first scanned a cohort of 27 non-contact-sport athletes ( $n=27$  males; range, 18–36 years; median, 28). Each registered brain voxel was assigned a value corresponding to a *normalized permeability*. Based on a cumulative distribution function (CDF) of normalized permeability values, we defined an upper limit for “normal” permeability as the 95th percentile of the mean CDF. Brain voxels with higher values were considered as having “*abnormally high permeability*.” An additional control group (healthy, non-athlete controls) recruited at a later stage ( $n=26$ ; range, 18–40 years; median, 30) as a test group. No differences in permeability maps were found between the two separate control groups.

Changes in DCE scan length were made given that the shorter scan time can sometimes inflate the laser Doppler microphone signal, because the length of time allowed for the contrast signal to decay following bolus injection until scan completion is less. To align scans with a previous study,<sup>20</sup> a longer scan time was utilized in the university rugby cohort and the MMA cohort. The values measured were normalized to an internal region of interest, and therefore relative values are used to generate % voxels. Also, there was no significant difference between the values generated using the shortened scan time and the longer scan time.

### Human plasma analyses

Immediately before undergoing an MRI scan, 16 mL of whole blood was withdrawn in  $K_2$  ethylenediminetetraacetic acid-coated tubes. Plasma and peripheral blood mononuclear cell (PBMC) fractions were separated by density fractionation. Briefly, whole-blood samples were diluted 1:1 with phosphate-buffered saline

TABLE 1.  $R^2$  OF THE LINEAR REGRESSION BETWEEN BRAIN DEFORMATION AND BBB DISRUPTION

Mechanical Fields	Impact Duration	Elements in Brain FEM Model	Average BBB Disruption (Slope)	Volume Fraction of BBB Disruption
1st Principal Strain, $\epsilon$	Integration, I	Total, $\Sigma$	0.81	0.89
		Average, A	0.44	0.53
		95%, 95	0.38	0.46
	Peak, P	Total, $\Sigma$	0.64	0.84
		Average, A	0.29	0.50
		95%, 95	0.28	0.52
1st Principal Strain Rate, $\dot{\epsilon}$	Integration, I	Total, $\Sigma$	0.84	0.96
		Average, A	0.52	0.68
		95%, 95	0.56	0.74
	Peak, P	Total, $\Sigma$	0.60	0.82
		Average, A	0.28	0.49
		95%, 95	0.29	0.52
1st Principal Stress, $\sigma$	Integration, I	Total, $\Sigma$	0.78	0.89
		Average, A	0.45	0.59
		95%, 95	0.41	0.53
	Peak, P	Total, $\Sigma$	0.41	0.67
		Average, A	0.22	0.46
		95%, 95	0.27	0.52
Power Absorbed, $\omega$	Integration, I	Total, $\Sigma$	0.23	0.25
		Average, A	0.20	0.22
		95%, 95	0.19	0.20
	Peak, P	Total, $\Sigma$	0.18	0.19
		Average, A	0.18	0.18
		95%, 95	0.17	0.17

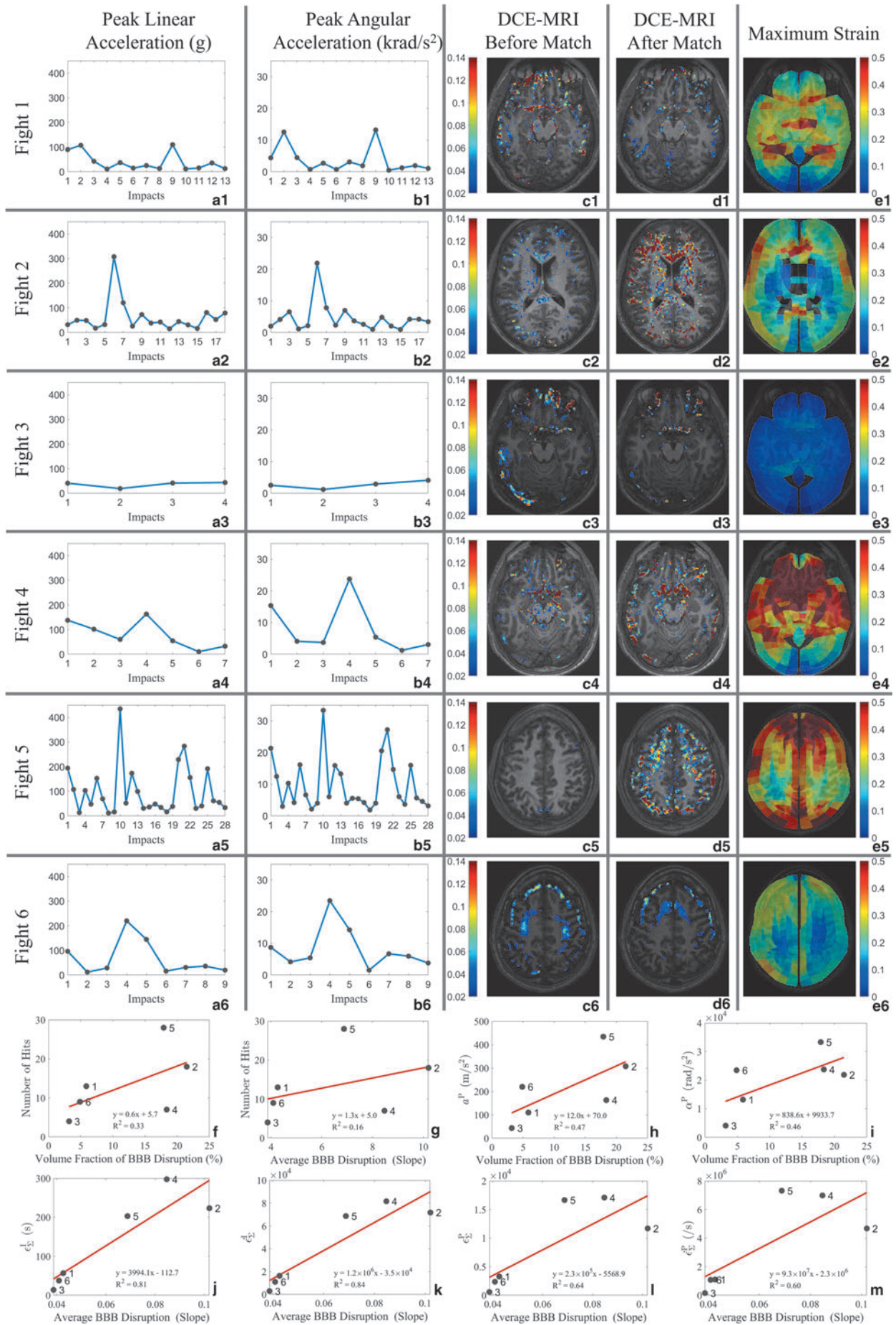
To describe the impact exposure, the mechanical fields from the simulation of each fight are based on 5 variables (time, impacts, and 3-dimensional space of brain). For each impact, at each voxel in the FEM model, we calculated the Integration (I) and Peak (P) of the mechanical parameters over time. Then, we took the maximum of these values over all recorded impacts for a given match. Lastly, over all 3-dimensional space, we computed the Total ( $\Sigma$ ), Average (A), 95% (95) over the mask of BBB disruption (the voxels where the slope is higher than the reported threshold [37] are selected) to represent the impact exposure as a single scalar value. The equations are given in Methods section (Eqs. 1–6). In DCE-MRI images, the average slope and volume fraction in the mask of BBB disruption were used to represent BBB disruption. For example, 0.81 is the  $R^2$  between and the average slope, and the linear regression is plotted in Fig.1J. (The color indicates the  $R^2$ , white is corresponding to  $R^2=0$  and red is corresponding to  $R^2 > 0.8$ )

before being layered on to 10 mL of Lymphoprep (STEMCELL Technologies, Vancouver, British Columbia, Canada). Samples were centrifuged at 400g for 45 min with 0 acceleration and deceleration to separate blood into plasma and PBMC fractions and stored at  $-80^\circ\text{C}$  until use.

Plasma brain-derived neurotrophic factor BDNF, monocyte chemoattractant protein 1/chemokine (C-C motif) ligand 2 (MCP1/CCL2), and S100 calcium binding protein B (S100B) levels were

measured using the Xmap (Luminex) method (R&D Systems, Minneapolis, USA) and enzyme-linked immunosorbent assay (ELISA; R&D Systems, Minneapolis, MN), per the manufacturer's instructions. In brief, the Luminex platform (consisting of the following analytes: BDNF, MCP-1/CCL2, S100B, interleukin [IL]-6, IL-18, IL-1beta, IL-33, IL-17A, IL-12 p70, IL-23, transforming growth factor-alpha, T-Tau, interferon-gamma, and glial fibrillary acidic protein) involved incubating diluted plasma samples (50  $\mu\text{L}$ )

**FIG. 1.** (A1–A6) Peak linear acceleration magnitude of the head measured by Stanford instrumented mouthguards (MiG 2.0) in professional mixed martial arts (MMA) fights 1–6 ( $n=5$  individual fighters). (B1–B6) Peak angular acceleration magnitude of head measured by the MiG 2.0 in professional mixed martial arts (MMA) fights 1–6. (C1–C6) Map of blood–brain barrier (BBB) disruption of the MMA fighters before the fights 1–6. (D1–D6) Map of BBB disruption of the MMA fighters after the matches 1–6. Both (C1–C6) and (D1–D6) were measured by DCE-MRI. (E1–E6) Map of peak deformation (first principal strain) during the fight. The deformations were obtained by assigning the kinematics measured during the fights to the KTH head model. The maximum deformations were selected among all impacts for every element independently. (F) Linear regression between the volume of BBB disruption (in %) and the total number of head impacts sustained during the fights. (G) Linear regression between the average BBB disruption (expressed as slope, in the mask of BBB disruption mask) and the total number of head impacts during the fights. (H) Linear regression between the volume of BBB disruption (in %) and the peak angular acceleration magnitude. (I) Linear regression between the volume of BBB disruption and the peak angular acceleration magnitude. (J) Linear regression between the average BBB disruption and  $\dot{\epsilon}_\Sigma^1$ . (K) Linear regression between the average BBB disruption and  $\dot{\epsilon}_\Sigma^1$ . (L) Linear regression between the average BBB disruption and  $\dot{\epsilon}_\Sigma^P$ . (M) Linear regression between the volume of BBB disruption and  $\dot{\epsilon}_\Sigma^P$ .



in a 96-well plate containing antibody-coated magnetic beads for 2 h at room temperature with gentle orbital agitation. After incubation, the beads were washed with the provided wash buffer and signal developed using the provided biotin antibody cocktail and streptavidin-peroxidase. Signal was determined using a Luminex 200 plate reader. Importantly, only levels of BDNF, MCP-1/CCL2, and S100B could be detected at sufficiently high levels and were subsequently chosen to confirm levels of expression using ELISA analysis.

For samples analysed using ELISA, plasma samples were incubated in individual 96-well plates coated with capture antibodies to human BDNF, MCP-1/CCL2, and S100B for 2 h at room temperature with gentle horizontal agitation. After incubation, plates were washed with the wash buffer and signal developed using the provided biotin-labeled antibody and streptavidin-peroxidase. Signal was determined using an ELISA plate reader. Levels of BDNF, MCP-1/CCL2, and S100B were calculated by a standard curve for each analyte. In two samples collected, hemolysis was present during collection and these were excluded from analysis.

### Statistical analyses

Statistical analysis was performed using Student's *t*-test, with significance represented by a *p* value of  $\leq 0.05$ . For multiple comparisons, analysis of variance (ANOVA) was used with a Tukey-Kramer post-test and significance represented by a *p* value of  $\leq 0.05$ . ANOVA, followed by a Bonferroni post-test, was used for multiple comparisons with  $p \leq 0.05$  representing significance. G\*Power was used *a priori* to calculate an appropriate sample size to ensure adequate power for experiments. For biomechanical regression with DCE-MRI results, multiple comparisons were made to look for correlations. Therefore, statistical significance is not considered in this analysis.

## Results

### Blood-brain barrier disruption is linked to repetitive traumatic brain injury

Using instrumented mouthguard technology (outlined in full in the Methods section), we investigated a link between single and repetitive TBIs and BBB disruption (Fig. 1). We recruited 5 professional MMA fighters to undergo pre-fight and post-fight testing and imaging (Fig. 1C,D). In combination, we instrumented the participants to measure TBI severity and exposure during fights (Fig. 1A). The number of impacts and the maximum head acceleration of these impacts were found to be in linear correlation to the volume fraction (Fig. 1F–H). We also used FE modeling to estimate brain tissue deformation produced by the TBIs (Fig. 1C). To investigate mechanical parameters correlating to BBB disruption, the first principal strain ( $\epsilon$ ), first principal strain rate ( $\dot{\epsilon}$ ), first principal stress ( $\sigma$ ), and the power absorbed ( $\omega$ ) were extracted from the simulation results. The mechanical parameters were correlated to the average slopes of contrast intensity and the fraction of volume where the BBB was disrupted, as shown in Table 1. Some of the linear regressions are plotted in Figure 1I–Q. For our cohort,  $\epsilon_{\Sigma}^1$ ,  $\dot{\epsilon}_{\Sigma}^1$ ,  $\sigma_{\Sigma}^1$  (Eq. 1) were in good correlation with both the average slope and BBB disruption volume fraction, and the  $\epsilon_{\Sigma}^p$ ,  $\dot{\epsilon}_{\Sigma}^p$  (Eq. 2) were only in good correlation with the BBB disruption volume fraction ( $R^2 > 0.80$ ). However, considering that only six data points were used in regression, these correlations need to be validated in the future. All parameters relating to the energy absorption were found to be poorly correlated to disruption of BBB. The maps of  $\epsilon^p$  were compared with the maps of BBB disruption locally (Fig. 1C);

however, the increased deformation was not locally associated with the increased changes of BBB.

### Blood-brain barrier disruption is evident in rugby players post-season

Using a weight-based bolus injection of Gadolinium and a dynamic contrast enhanced MRI (DCE-MRI) paradigm,<sup>26</sup> we were able to measure BBB integrity in rugby players examined pre-season (before regular full contact training and competition) and again at a return imaging session after conclusion of the rugby season (Fig. 2A). With a sample size of 19, there were no overall differences in gadolinium signal when pre-season scans were compared to post-season scans across the entire group (Fig. 2B). However, increases in signal post-season when compared to pre-season were observed in the periventricular regions of the brain in 10 of 19 subjects who completed the study (Fig. 2C). Indeed, when the BBB-disrupted voxels across the entire groups were examined at pre-season compared to post-season, it was evident that a subgroup of individuals displayed increased BBB disruption post-season compared to their pre-season scan (Fig. 2D). This BBB disruption was significantly increased in this subgroup of players (Fig. 2E).

Systemic biomarkers of BBB damage and brain trauma have been purported to have utility in determining prognosis post-TBI. In this regard, we screened plasma samples from participants pre-season and post-season in an effort to examine the differential expression of 14 common TBI biomarkers. Of these (outlined in full in the Methods section), only two were detectable at sufficiently high levels to be quantified. Levels of BDNF (Fig. 2F) were significantly increased in subjects post-season compared to plasma levels pre-season (\*\* $p = 0.004$ ). No differences were observed in levels of MCP-1 (Fig. 2G). Levels of the commonly used BBB disruption biomarker, S100B, surprisingly decreased in plasma samples post-season compared to pre-season (\* $p < 0.05$ ; Fig. 2H). There was only a very weak correlation of S100B levels with the % disrupted voxels, but this was a negative correlation (Supplementary Fig. S1).

### Blood-brain barrier disruption in the acute stages post-match

Whereas BBB disruption and differential levels of biomarkers were evident in analyses of pre-season versus post-season school-boy rugby players, we wished to ascertain whether this BBB disruption was occurring in the acute phases post-exposure to repetitive TBI. In this regard, we recruited a subgroup of university-based rugby union players (ages 18–23 years). In this group, we enrolled 8 participants to undergo pre-season testing and imaging. Using the linear method of DCE-MRI analysis, 2 of 8 subjects had an increased signal intensity post-match compared to their pre-season scan (Fig. 3A), one of which returned to baseline at the end of the season (Fig. 3C), showing reversibility of the BBB disruption, whereas the other manifested a higher signal post-season.

Unlike the pre-season/post-season analyses, examining levels of BDNF in participants did not show any difference in plasma levels post-match compared to pre-season (Fig. 3C); however, levels of MCP-1 were significantly increased post-match in this group (\* $p = 0.012$ ; Fig. 3D). Interestingly, and as has been reported previously, S100B levels were also shown to increase significantly post-match (\* $p = 0.01$ ; Fig. 3E). There was weak positive correlation between S100B levels and % disrupted voxel increases (Supplementary Fig. S1). The demographics of rugby players and MMA

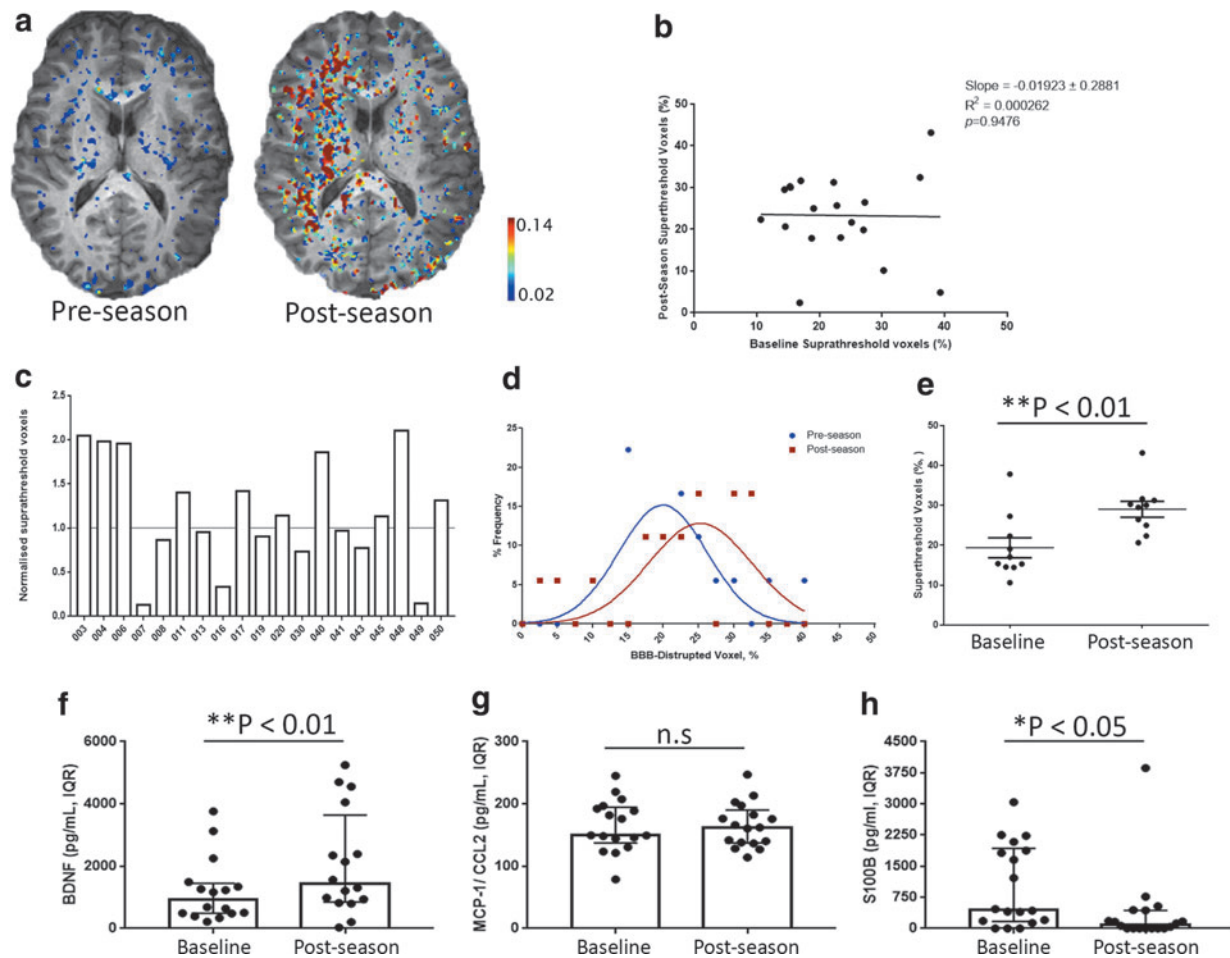


**FIG. 2.** (A) Enhanced gadolinium contrast agent (red) observed post-season in a youth rugby player (linear method). (B) Linear regression between BBB disruption volume (in % voxels) at baseline versus post-season ( $n = 19$ ). (C) Relative to baseline changes in volume of BBB disruption post-season ( $n = 19$ ). (D) Distribution frequency of volume of BBB disruption (in % voxels) in players pre-season and post-season to ( $n = 19$ ). (E) Increased BBB disruption volume (in % voxels) in players post-season compared to matched pre-season (\*\* $p < 0.001$ ;  $n = 9$ ). (F) Brain-derived neurotrophic factor (BDNF) levels are significantly increased in players plasma post-season compared to pre-season (\*\* $p = 0.004$ ;  $n = 16$ ). (G) Monocyte chemoattractant protein-1 (MCP-1) levels are significantly increased in players plasma post-season compared to pre-season (\* $p = 0.01$ ;  $n = 17$ ). (H) Decreased levels of S100B detectable post-season compared to pre-season ( $p < 0.05$ ), ( $n = 17$ ). BBB, blood–brain barrier; CCL2, C-C motif chemokine ligand 2; IQR, interquartile range; n.s., not significant; S100B, S100 calcium-binding protein B.

fighters who participated in our study are outlined in Supplementary Figure S2.

## Discussion

Our pilot study provides the first analysis of BBB function in a group of MMA fighters and rugby players exposed to varying levels of repetitive TBI in the context of playing competitive contact sports. Taken together, our data suggest that dynamic changes to the BBB may occur after a full season of contact sport, with these changes manifesting in up to 52% of adolescents. Although there were slight modifications to the MRI scanning parameters between the schoolboy rugby study and the university rugby study/MMA study, we observed no significant differences between the values generated. Additionally, the pattern of BDNF, MCP-1, and S100B, biomarkers detected post-season and post-match, suggest that these markers may aid in the indication of subconcussive trauma and, possibly, also inform in return to baseline assessments. Importantly, however, it appears that these biomarkers may have

limited utility as “stand-alone” readouts given that we observed decreased levels of S100B in blood of players after a full season of rugby. The elusive temporal profile of these biomarkers after trauma also makes it challenging to use solely as a biomarker of brain injury.

From animal TBI models, it is suggested that TBI may cause primary damage to the brain parenchyma leading to BBB pathophysiology and CTE.<sup>13,27</sup> From the field of ultrasound-assisted drug delivery, it is well known that mechanical forces open the BBB complex in humans and result in inflammation. However, animal studies do not necessarily recapitulate the tissue-level biomechanical forces experienced by humans in sports, so it is unknown whether BBB disruption and inflammation occur in child or adult athletes. In this regard, in our study we measured the kinematics of head hits sustained by 5 professional MMA fighters who also underwent pre-fight and post-fight testing and imaging in six fights (Fig. 1; fight 3 and 6 are same fighter). Although all 5 fighters were concussed, we found a wide spectrum of BBB integrity. Based on these pilot data (Table 1), we found that several

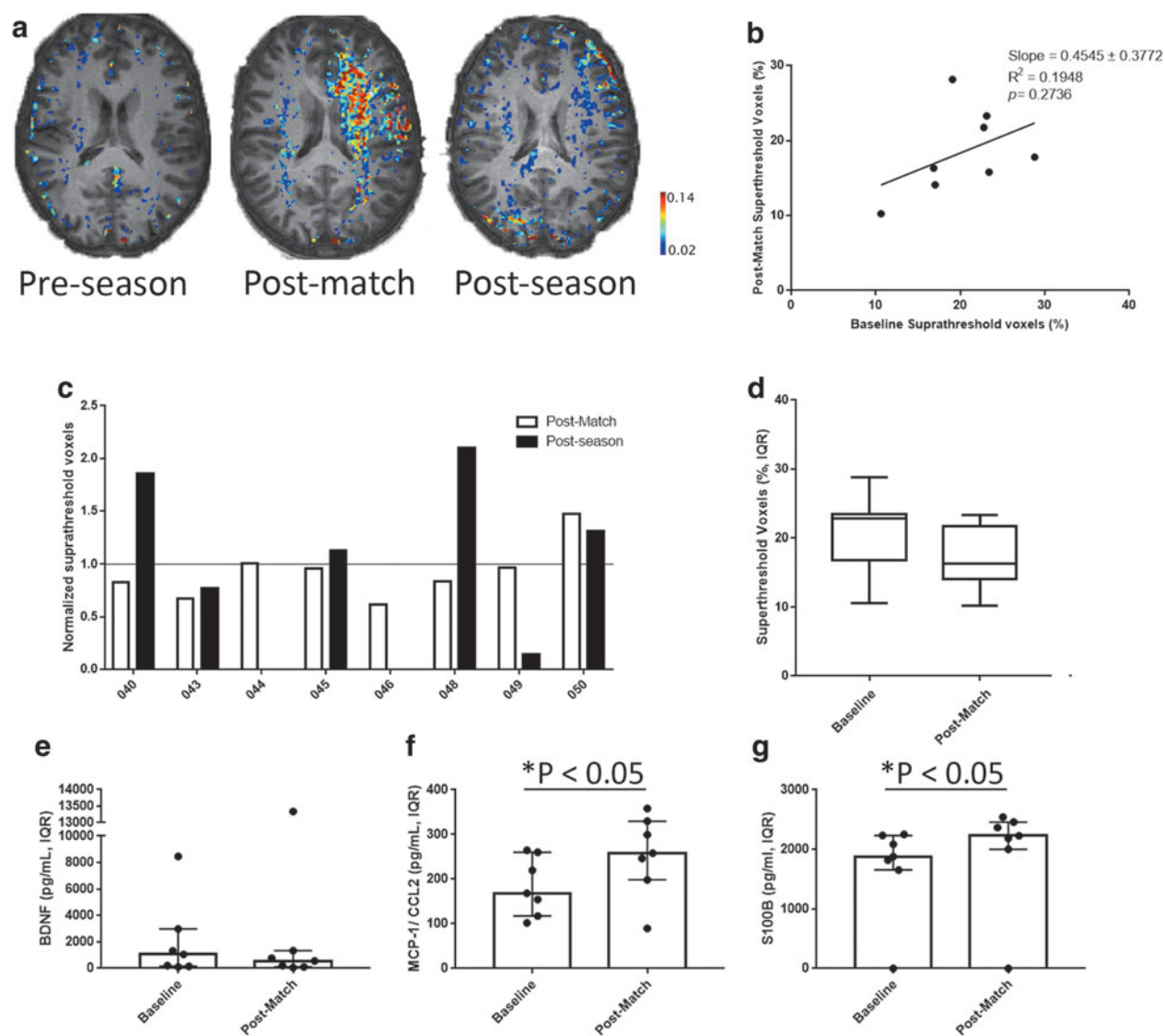


**FIG. 3.** (A) Enhanced gadolinium contrast agent (red) observed post-match and post-season in a university-level rugby player (linear method). (B) Linear regression between BBB disruption volume (in % voxels) at baseline versus post-match ( $n=8$ ). (C) Relative to baseline changes in volume of BBB disruption post-match and post-season ( $n=8$ ). (D) Non-significant changes in BBB disruption volume (in % voxels) post-match compared to baseline. (E) Brain-derived neurotrophic factor (BDNF) levels pre-season compared to post-match ( $n=7$ ). (F) Increased levels of monocyte chemoattractant protein-1 (MCP-1) post-match compared to pre-season ( $*p=0.012$ ;  $n=7$ ). (G) Increased levels of S100B observed post-match compared to pre-season ( $*p=0.01$ ;  $n=7$ ). BBB, blood-brain barrier; CCL2, C-C motif chemokine ligand 2; IQR, interquartile range; S100B, S100 calcium-binding protein B.

mechanical parameters were well correlated to the BBB disruption, indicating that these parameters could have potentially candidates to induce the dysfunction. Interestingly, we found the Integration (I) of parameters over time always had higher correlations than taking the Peak (P), which suggests that the deformation time history may affect BBB opening. In our analysis, the maximum mechanical parameters over all impacts, for every voxel of the brain, were found to correlate with BBB disruption. This correlation assumes that the BBB disruption in one voxel was determined by the most severe deformation among all impacts; this final deformation at each point in 3D space may not be caused by the same impact. This suggests that, as a fighter experiences additional impacts within a fight, this has the potential to lead to increased BBB disruption if more parts of the brain experience higher mechanical deformations. However, the cumulative effect of the deformation

between impacts was not strictly considered in this analysis. Further, owing to the different geometry and the low resolution of the FE head model, the maps of the mechanical parameter could not be associated with the BBB disruption locally.

In the subject who was knocked out within the first 2 min of the fight (Fig. 1C, figure 3), we found little evidence of BBB disruption even after a transient loss of consciousness. However, upon inspecting the mouthguard data, we found relatively low accelerations (four impacts all  $<50$  gs and  $5000$  rad/s<sup>2</sup>) and small brain strains from FE modeling ( $<10\%$  maximum principal strain). Although the study sample is too small for conclusive findings, the weaker correlation between number of impacts and BBB disruption brings into question the theory that sub-concussive impacts accumulate within a single match to cause more severe brain injury. However, our data does suggest that multiple

impacts in a single match leads to more parts of the brain affected, which is distinct from increasing the severity in a given brain region. Because this analysis was only done on a single fight, this simultaneous correlation of severity of hits we observed in concussed professional fighters leaves open the question as to what effect repetitive subconcussive exposure and BBB disruptions may have over long time periods on its own.

In the context of moderate or severe TBI, it is known that BBB disruption is an early event that can persist for years and decades after the initial injury.<sup>28,29</sup> It is of major interest that the end-stage pathology observed in CTE appears to be a terminal disruption and dysfunction in the integrity of the BBB in areas of dense perivascular P-Tau deposition.<sup>11</sup> In CTE, it is tempting to suggest that repetitive exposure to TBI, as observed in a subset of players in our study, without allowing sufficient time for BBB recovery, will lead to long-term and persistent BBB disruption and therefore to the long-term sequelae associated with some forms of mTBI.<sup>30,31</sup> In animal studies, such prolonged BBB disruption is associated with neuroinflammation and pathological synaptogenesis, plasticity, and hence abnormal network activity.<sup>13</sup>

Although our study cannot speak pervasively to concussive brain injuries *per se*, we have highlighted that the very nature of contact sports as violent as MMA and as typical as rugby can manifest dynamic changes to the integrity and regulation of the BBB attributable to what we can term subconcussive events.

The current clinical assessment of mTBI falls far below the kind of objective criteria that would provide meaningful and clinically robust diagnostic and prognosis information for patients. This is compounded not only by the lack of an appropriate imaging paradigm, but also attributable to the lack of any systemic biomarkers that can predict the severity of injury. Lately, there has been a growing awareness of implications of concussive brain injuries in sports given the well-defined increased risk of dementia associated with moderate or severe TBI<sup>32–36</sup> and emerging evidence suggestive of a link between repetitive mTBI and the development of CTE.<sup>37–39</sup> There is a clear need for understanding the molecular etiology of concussive and subconcussive brain injuries and for developing methods to aid in the diagnosis and management of such injuries to the brain.

Although participation in sports activities is hugely important for social, physiological, and psychological development of children and young adults, it is critical that we make objective and rational decisions on a case-by-case basis when deciding whether athletes should compete in full contact sports. The most common contact sports include rugby, American football, boxing, horse riding, and MMA. What remains to be elucidated, however, is whether these sports are putting future brain health at an acceptable risk. Expanded and longitudinal studies using the multi-disciplinary methods outlined in the current pilot study will undoubtedly lead to better management and clinical decision making with regard to repetitive mTBI. Imaging of BBB integrity in tandem with serological analysis of participants in contact sports could also form the central platform in diagnosis and may better inform return-to-play guidelines.

## Acknowledgments

We thank Caroline Woods and Charles Murray for animal husbandry.

## Author Contributions

E.O.K. analyzed MRI data. E.K. performed clinical workup of participants. C.G. performed instrumented mouthguard analysis.

E.W. and A.H. performed clinical workup of participants. C.G. analyzed data. S.T. and A.M. performed instrumented mouthguard analysis. S.H. performed data collection. T.B. analyzed data. J.K. performed data collection. N.D. performed Data collection. G.A.G. performed MRI analysis and design. A.F. performed MRI analysis and design. R.V. performed MRI analysis and design. M.G.M. conceived experiments. J.F.M. conceived MRI experiments. N.P. conceived experiments. D.C. performed instrumented mouthguard analysis. C.D. conceived, designed, and performed experiments, analyzed data, and wrote the manuscript. M.C. conceived, designed, and performed experiments, analyzed data, and wrote the manuscript.

## Funding Information

This work was supported by grants from Science Foundation Ireland (SFI; 12/YI/B2614 and 11/PI/1080), The Health Research Board of Ireland (HRB), the BrightFocus Foundation, and the St James' Hospital Foundation with support to E.K. from the Ellen Mayston Bates Bequest at the Trinity Foundation. The Campbell lab at TCD is also supported by an SFI Centres grant supported, in part, by a research grant from SFI under grant number 16/RC/3948 and co-funded under the European Regional Development fund by FutureNeuro industry partners. Work in the laboratory of A.F. is supported by the Canada Institute for Health Research (CIHR; to A.F.).

## Author Disclosure Statement

No competing financial interests exist.

## References

1. Roozenbeek, B., Maas, A.I.R., and Menon, D.K. (2013). Changing patterns in the epidemiology of traumatic brain injury. *Nat. Rev. Neurol.* 9, 231–236.
2. Helmy, A., Vizcaychipi, M., and Gupta, A.K. (2007). Traumatic brain injury: intensive care management. *Br. J. Anaesth.* 99, 32–42.
3. Stokum, J.A., Gerzanich, V., and Simard, J.M. (2016). Molecular pathophysiology of cerebral edema. *J. Cereb. Blood Flow Metab.* 36, 513–538.
4. Montenegro, P.H., Alosco, M.L., Martin, B.M., Daneshvar, D.H., Mez, J., Chaisson, C.E., Nowinski, C.J., Au, R., McKee, A.C., Cantu, R.C., McClean, M.D., Stern, R.A., and Tripodis, Y. (2017). Cumulative head impact exposure predicts later-life depression, apathy, executive dysfunction, and cognitive impairment in former high school and college football players. *J. Neurotrauma* 34, 328–340.
5. McCrory, P., Meeuwisse, W., Dvorak, J., Aubry, M., Bailes, J., Broglio, S., Cantu, R.C., Cassidy, D., Echemendia, R.J., Castellani, R.J., Davis, G.A., Ellenbogen, R., Emery, C., Engebretsen, L., Feddermann-Demont, N., Giza, C.C., Guskiewicz, K.M., Herring, S., Iverson, G.L., Johnston, K.M., Kissick, J., Kutcher, J., Leddy, J.J., Maddocks, D., Makdissi, M., Manley, G.T., McCrea, M., Meehan, W.P., Nagahiro, S., Patricios, J., Putukian, M., Schneider, K.J., Sills, A., Tator, C.H., Turner, M., and Vos, P.E. (2017). Consensus statement on concussion in sport—the 5th international conference on concussion in sport held in Berlin, October 2016. *Br. J. Sports Med.* 51, 838–847.
6. Lynall, R.C., Campbell, K.R., Wasserman, E.B., Dompier, T.P., and Kerr, Z. (2017). Concussion mechanisms and activities in youth, high school, and college football. *J. Neurotrauma* 34, 2684–2690.
7. McMillan, T.M., McSkimming, P., Wainman-Lefley, J., Maclean, L.M., Hay, J., McConnachie, A., and Stewart, W. (2017). Long-term health outcomes after exposure to repeated concussion in elite level: rugby union players. *J. Neurol. Neurosurg. Psychiatry* 88, 505–511.
8. Purcell, L.K., and Leblanc, C.M.; Canadian Paediatric Society, Healthy Active Living and Sports Medicine Committee, and American Academy of Pediatrics, Council on Sports Medicine and Fitness. (2012). Boxing participation by children and adolescents: a joint statement with the American Academy of Pediatrics. *J. Paediatr. Child Health* 17, 39–40.

9. Koerte, I.K., Nichols, E., Tripodis, Y., Schultz, V., Lehner, S., Igbonoba, R., Chuang, A.Z., Mayinger, M., Klier, E.M., Muehlmann, M., Kaufmann, D., Lepage, C., Heinen, F., Schulte-Körne, G., Zafonte, R., Shenton, M.E., and Sereno, A.B. (2017). Impaired cognitive performance in youth athletes exposed to repetitive head impacts. *J. Neurotrauma* 34, 2389–2395.
10. Mez, J., Solomon, T.M., Daneshvar, D.H., Murphy, L., Kiernan, P.T., Montenigro, P.H., Kriegel, J., Abdolmohammadi, B., Fry, B., Babcock, K.J., Adams, J.W., Bourlas, A.P., Papadopoulos, Z., McHale, L., Ardaugh, B.M., Martin, B.R., Dixon, D., Nowinski, C.J., Chaisson, C., Alvarez, V.E., Tripodis, Y., Stein, T.D., Goldstein, L.E., Katz, D.I., Kowall, N.W., Cantu, R.C., Stern, R.A., and McKee, A.C. (2015). Assessing clinicopathological correlation in chronic traumatic encephalopathy: rationale and methods for the UNITE study. *Alzheimers Res. Ther.* 7, 62.
11. Smith, D.H., Johnson, V.E., Trojanowski, J.Q., and Stewart, W. (2019). Chronic traumatic encephalopathy—confusion and controversies. *Nat. Rev. Neurol.* 15, 179–183.
12. Doherty, C.P., O'Keefe, E., Wallace, E., Loftus, T., Keaney, J., Kealy, J., Humphries, M.M., Molloy, M.G., Meaney, J.F., Farrell, M., and Campbell, M. (2016). Blood-brain barrier dysfunction as a hallmark pathology in chronic traumatic encephalopathy. *J. Neuropathol. Exp. Neurol.* 75, 656–662.
13. Tagge, C.A., Fisher, A.M., Minaeva, O.V., Gaudreau-Balderrama, A., Moncaster, J.A., Zhang, X.L., Wojnarowicz, M.W., Casey, N., Lu, H., Kokiko-Cochran, O.N., Saman, S., Ericsson, M., Onos, K.D., Veksler, R., Senatorov, V.V., Jr., Kondo, A., Zhou, X.Z., Miry, O., Vose, L.R., Gopaul, K.R., Upreti, C., Nowinski, C.J., Cantu, R.C., Alvarez, V.E., Hildebrandt, A.M., Franz, E.S., Konrad, J., Hamilton, J.A., Hua, N., Tripodis, Y., Anderson, A.T., Howell, G.R., Kaufer, D., Hall, G.F., Lu, K.P., Ransohoff, R.M., Cleveland, R.O., Kowall, N.W., Stein, T.D., Lamb, B.T., Huber, B.R., Moss, W.C., Friedman, A., Stanton, P.K., McKee, A.C., and Goldstein, L.E. (2018). Concussion, microvascular injury, and early tauopathy in young athletes after impact head injury and an impact concussion mouse model. *Brain* 141, 422–458.
14. Abbott, N.J., Patabendige, A.A., Dolman, D.E., Yusof, S.R., and Begley, D.J. (2010). Structure and function of the blood-brain barrier. *Neurobiol. Dis.* 37, 13–25.
15. Abbott, N.J., Ronnback, L., and Hansson, E. (2006). Astrocyte-endothelial interactions at the blood-brain barrier. *Nat. Rev. Neurosci.* 7, 41–53.
16. Pardridge, W.M. (2005). The blood-brain barrier: bottleneck in brain drug development. *NeuroRx* 2, 3–14.
17. Hawkins, B.T., and Davis, T.P. (2005). The blood-brain barrier/neurovascular unit in health and disease. *Pharmacol. Rev.* 57, 173–185.
18. Obermeier, B., Daneman, R., and Ransohoff, R.M. (2013). Development, maintenance and disruption of the blood-brain barrier. *Nat. Med.* 19, 1584–1596.
19. Wu, L.C., Nangia, V., Bui, K., Hammor, B., Kurt, M., Hernandez, F., Kuo, C., and Camarillo, D.B. (2016). In vivo evaluation of wearable head impact sensors. *Ann. Biomed. Eng.* 44, 1234–1245.
20. Kuo, C., Wu, L.C., Hammor, B.T., Luck, J.F., Cutcliffe, H.C., Lynnall, R.C., Kait, J.R., Campbell, K.R., Mihalik, J.P., Bass, C.R., and Camarillo, D.B. (2016). Effect of the mandible on mouthguard measurements of head kinematics. *J. Biomech.* 49, 1845–1853.
21. Hernandez, F., Wu, L.C., Yip, M.C., Laksari, K., Hoffman, A.R., Lopez, J.R., Grant, G.A., Kleiven, S., and Camarillo, D.B. (2015). Six degree-of-freedom measurements of human mild traumatic brain injury. *Ann. Biomed. Eng.* 43, 1918–1934.
22. Kleiven, S. (2007). Predictors for traumatic brain injuries evaluated through accident reconstructions. *Stapp Car Crash J.* 51, 81–114.
23. Hardy, W. (2001). Investigation of head injury mechanisms using neutral density technology and high-speed biplanar x-ray. *Stapp Car Crash J.* 45, 337–368.
24. Hardy, W.N., Mason, M.J., Foster, C.D., Shah, C.S., Kopacz, J.M., Yang, K.H., King, A.I., Bishop, J., Bey, M., Anderst, W., and Tashman, S. (2008). A study of the response of the human cadaver head to impact. *Stapp Car Crash J.* 51, 17–80.
25. Weissberg, I., Veksler, R., Kamintsky, L., Saar-Ashkenazy, R., Miliukovsky, D.Z., Shelef, I., and Friedman, A. (2014). Imaging blood-brain barrier dysfunction in football players. *JAMA Neurol.* 71, 1453–1455.
26. Veksler, R., Shelef, I., and Friedman, A. (2014). Blood-brain barrier imaging in human neuropathologies. *Arch. Med. Res.* 45, 646–652.
27. Johnson, V.E., Weber, M.T., Xiao, R., Cullen, D.K., Meaney, D.F., Stewart, W., and Smith, D.H. (2018). Mechanical disruption of the blood-brain barrier following experimental concussion. *Acta Neuropathol.* 135, 711–726.
28. Hay, J.R., Johnson, V.E., Young, A.M., Smith, D.H., and Stewart, W. (2015). Blood-brain barrier disruption is an early event that may persist for many years after traumatic brain injury in humans. *J. Neuropathol. Exp. Neurol.* 74, 1147–1157.
29. Doherty, C.P., O'Keefe, E., Keaney, J., Lawlor, B., Coen, R.F., Farrell, M., and Campbell, M. (2019). Neuropathology as a result of severe traumatic brain injury? *Clin. Neuropathol.* 38, 14–22.
30. Greene, C., Kealy, J., Humphries, M.M., Gong, Y., Hou, J., Hudson, N., Cassidy, L.M., Martiniano, R., Shashi, V., Hooper, S.R., Grant, G.A., Kenna, P.F., Norris, K., Callaghan, C.K., Islam, M.N., O'Mara, S.M., Najda, Z., Campbell, S.G., Pachter, J.S., Thomas, J., Williams, N.M., Humphries, P., Murphy, K.C., and Campbell, M. (2018). Dose dependent expression of claudin-5 is a modifying factor in schizophrenia. *Mol. Psychiatry* 23, 2156–2166.
31. Menard, C., Pfau, M.L., Hodes, G.E., Kana, V., Wang, V.X., Bouchard, S., Takahashi, A., Flanigan, M.E., Aleyasin, H., LeClair, K.B., Janssen, W.G., Labonté, B., Parise, E.M., Lorsch, Z.S., Golden, S.A., Heshmati, M., Tamminga, C., Turecki, G., Campbell, M., Fayad, Z.A., Tang, C.Y., Merad, M., and Russo, S.J. (2017). Social stress induces neurovascular pathology promoting depression. *Nat. Neurosci.* 20, 1752–1760.
32. Nitta, T., Hata, M., Gotoh, S., Seo, Y., Sasaki, H., Hashimoto, N., Furuse, M., and Tsukita, S. (2003). Size-selective loosening of the blood-brain barrier in claudin-5-deficient mice. *J. Cell Biol.* 161, 653–660.
33. Ojo, J.O., Mouzon, B., Algamal, M., Leary, P., Lynch, C., Abdullah, L., Evans, J., Mullan, M., Bachmeier, C., Stewart, W., and Crawford, F. (2016). Chronic repetitive mild traumatic brain injury results in reduced cerebral blood flow, axonal injury, gliosis, and increased T-tau and tau oligomers. *J. Neuropathol. Exp. Neurol.* 75, 636–655.
34. Mortimer, J.A., van Duijn, C.M., Chandra, V., Fratiglioni, L., Graves, A.B., Heyman, A., Jorm, A.F., Kokmen, E., Kondo, K., and Rocca, W.A. (1991). Head trauma as a risk factor for Alzheimer's disease: a collaborative re-analysis of case-control studies. EURODEM Risk Factors Research Group. *Int. J. Epidemiol.* 20, Suppl. 2, S28–S35.
35. Fleminger, S., Oliver, D.L., Lovestone, S., Rabe-Hesketh, S., and Giora, A. (2003). Head injury as a risk factor for Alzheimer's disease: the evidence 10 years on; a partial replication. *J. Neurol. Neurosurg. Psychiatry* 74, 857–862.
36. Gardner, R.C., Burke, J.F., Nettiksimmons, J., Kaup, A., Barnes, D.E., and Yaffe, K. (2014). Dementia risk after traumatic brain injury vs nonbrain trauma: the role of age and severity. *JAMA Neurol.* 71, 1490–1497.
37. Stewart, W., McNamara, P.H., Lawlor, B., Hutchinson, S., and Farrell, M. (2016). Chronic traumatic encephalopathy: a potential late and under recognized consequence of rugby union? *QJM* 109, 11–15.
38. Iacono, D., Shively, S.B., Edlow, B.L., and Perl, D.P. (2017). Chronic traumatic encephalopathy: known causes, unknown effects. *Phys. Med. Rehabil. Clin. N. Am.* 28, 301–321.
39. McKee, A.C., Cairns, N.J., Dickson, D.W., Folkerth, R.D., Keene, C.D., Litvan, I., Perl, D.P., Stein, T.D., Vonsattel, J.P., Stewart, W., Tripodis, Y., Crary, J.F., Bieniek, K.F., Dams-O'Connor, K., Alvarez, V.E., and Gordon, W.A.; TBI/CTE group. (2016). The first NINDS/NIBIB consensus meeting to define neuropathological criteria for the diagnosis of chronic traumatic encephalopathy. *Acta Neuropathol.* 131, 75–86.

Address correspondence to:  
 Matthew Campbell, PhD  
 Smurfit Institute of Genetics  
 Trinity College Dublin  
 Lincoln Place Gate  
 Dublin 2  
 Ireland

E-mail: Matthew.Campbell@tcd.ie